

Ground state and edge excitations of quantum Hall liquid at filling factor 2/3

Zi-Xiang Hu,^{1,2} Hua Chen,¹ Kun Yang,² E. H. Rezayi,³ and Xin Wan⁴

¹*Zhejiang Institute of Modern Physics, Zhejiang University, Hangzhou 310027, P.R. China*

²*National High Magnetic Field Laboratory and Department of Physics,
Florida State University, Tallahassee, Florida 32306, USA*

³*Department of Physics, California State University Los Angeles, Los Angeles, California 90032, USA*

⁴*Asia Pacific Center for Theoretical Physics and Department of Physics,
Pohang University of Science and Technology, Pohang, Gyeongbuk 790-784, Korea*

(Dated: October 31, 2018)

We present a numerical study of fractional quantum Hall liquid at Landau level filling factor $\nu = 2/3$ in a microscopic model including long-range Coulomb interaction and edge confining potential, based on the disc geometry. We find the ground state is accurately described by the particle-hole conjugate of a $\nu = 1/3$ Laughlin state. We also find there are two counter-propagating edge modes, and the velocity of the forward-propagating mode is larger than the backward-propagating mode. The velocities have opposite responses to the change of the background confinement potential. On the other hand changing the two-body Coulomb potential has qualitatively the same effect on the velocities; for example we find increasing layer thickness (which softens of the Coulomb interaction) reduces both the forward mode and the backward mode velocities.

PACS numbers:

I. INTRODUCTION

The fractional quantum Hall (FQH) effect is a remarkable phenomenon observed in two-dimensional electron gases (2DEGs) in a strong perpendicular magnetic field. FQH liquids are gapped and believed to possess topological order.¹ In particular, it has been established that the $\nu = 1/3$ Laughlin state represents an Abelian topological phase. The excitations in such a phase can carry a fraction of electron charge and have fractional statistics which are in-between bosonic and fermionic statistics. Various experiments have reported observation of fractional charge^{2,3,4}. Recently, a series of experiments^{5,6} observed the so-called superperiods in the conductance oscillations in an FQH quasiparticle interferometer, which have been interpreted as a reflection of fractional statistics.^{7,8} The bulk topological order is also reflected in the corresponding edge excitations, which are gapless. For a $\nu = 1/3$ FQH liquid, with a sharp confining potential (no edge reconstruction), there is only a single branch of bosonic excitations at the edge. The bosonic edge mode is chiral, i.e., propagating along the edge in one direction (determined by the $\mathbf{E} \times \mathbf{B}$ drift) only, because the magnetic field breaks the time-reversal symmetry. The edge physics can be described by the chiral Luttinger liquid theory and has been verified by numerical tests in microscopic models.^{9,10}

In a hierarchical state, the FQH liquid supports multiple branches of edge excitations. Depending on the bulk topological order, the edge modes may propagate in the same direction or in opposite directions. The simplest case with counter-propagating edge modes is the spin-polarized FQH liquid at filling fraction $\nu = 2/3$, which can be regarded as the particle-hole conjugate of a $\nu = 1/3$ Laughlin state or, equivalently, a hole Laughlin state embedded in a $\nu = 1$ integer quantum Hall back-

ground (see Fig. 1 for an illustration).^{11,12,13} Roughly speaking, the inner and outer edges are located at density changes of $2/3 \rightarrow 1$ and $1 \rightarrow 0$, respectively. In general, the two edge modes are coupled to each other and their properties may be dominated by disorder in the presence of random edge tunneling.^{14,15} The edge physics of the $\nu = 2/3$ state is intriguing since one of the edge modes propagates opposite to the classical skipping orbits dictated by the uniform magnetic field, leading to a negative contribution to thermal Hall conductivity.¹⁶ The counter-propagating edge modes have since been studied^{17,18,19,20,21} both theoretically and experimentally in recent years.

Recently, a similar but more delicate situation arises at filling fraction $\nu = 5/2$, where the Moore-Read Pfaffian state²² and its particle-hole conjugated state, dubbed the anti-Pfaffian state,^{23,24} compete for the ground state. In the absence of Landau level mixing, impurity, or edge confinement, the particle-hole symmetry is unbroken. In this case the two states, in the bulk, are expected to be degenerate in the thermodynamic limit. But these two states have very different edge structures: the Pfaffian state supports two co-propagating chiral edge modes (a charged bosonic mode and a neutral fermionic mode), while the anti-Pfaffian state supports three counter-propagating charge and neutral modes.^{23,24} Their relation is somewhat similar to that between the $\nu = 1/3$ and $\nu = 2/3$ edge states. We note very recent experiments^{25,26,27} found indications of quasiparticle excitations with charge $e/4$ supported by both states and, interestingly, tunneling experiments²⁶ seem to favor the anti-Pfaffian state over the Pfaffian state. We also note that the particle-hole conjugates of the Read-Rezayi state²⁸ have been studied theoretically, with emphasis on properties of their edge excitations.²⁹

Motivated by the recent work on the particle-hole con-

jugate of the Pfaffian state^{23,24} and Read-Rezayi states,²⁹ as well as by the experimental measurement of the $I-V$ spectroscopy between individual edge channels,³⁰ we revisit the polarized $\nu = 2/3$ FQH state with a detailed numerical study on the edge modes of the $\nu = 2/3$ FQH droplet using a semi-realistic microscopic model. We find the ground states of the system for a wide parameter range are well described by the composite of a $\nu = 1$ IQH droplet and a $\nu = 1/3$ Laughlin hole droplet. The number of electrons and holes in the two droplets vary as the strength of confining potential varies, under the constraint that the total number of electrons does not change. Two counter-propagating edge modes are clearly visible in our results. Quantitatively, we find the forward-propagating outer edge mode (arising from the IQH edge) has a larger velocity than that of the backward-propagating inner edge (from the hole FQH edge). The structure of the excitation spectrum of the inner edge is identical to that of the Laughlin state at $\nu = 1/3$ except for direction of propagation. Increasing the edge confining potential increases the outer edge mode velocity and *reduces* the inner edge mode velocity. We also carry out a particle-hole transformation of the electronic Hamiltonian with hard-core interaction to generate the Hamiltonian that makes the hole Laughlin state and hole edge states as its exact zero-energy ground states. Using a mixed Hamiltonian which contains both the electron Coulomb Hamiltonian and the the conjugate Hamiltonian of the two-body hard-core interaction, the bulk excitation energies can be raised to allow for a clearer separation between bulk and edge excitations. We find our results are robust in the presence of the electronic layer thickness, whose main effect is softening the Coulomb interaction and reducing the velocities of both edge modes.

The rest of the paper is organized as follows. In Sec. II we describe the microscopic model used in this work. We discuss the nature of the ground states in Sec. III. We present the overlap study of the ground states with variational wave functions in Sec. IV. A detailed analysis of the edge states follows in Sec. V. One can find explicit construction of the Hamiltonian for the variational wave functions of the ground states and edge states in Sec. VI. We consider the effect of electron layer thickness in Sec. VII and quasihole excitations in Sec. VIII. Finally, some concluding remarks are offered in Sec. IX.

II. THE MODEL

In recent years, we have developed a semi-realistic microscopic model for FQH liquids and have studied edge excitations and instabilities, quasihole/quasiparticle excitations, and edge tunneling in Laughlin and Moore-Read Pfaffian phases.^{10,31,32,33,34,35} The advantage of the model is that, depending on the parameters, the Laughlin phase, the Moore-Read phase, as well as edge reconstructed states and quasihole/quasiparticle states,

emerge naturally as the global ground state of the microscopic Hamiltonian without any explicit assumptions, e.g., on the value of the ground state angular momentum. This way, we can study the stability of phases and their competition. Another advantage of the model is that we can analyze the edge excitations of the semi-realistic system and identify them in a one-to-one correspondence with edge excitations of the corresponding edge theory (or conformal field theory). In addition to confirming the bulk topological order, we can use the microscopic calculation to extract energetic quantities, such as edge velocities, which are crucial for quantitative comparisons with experiments; for example in a recent study we used the edge mode velocities extracted from our numerical study to estimate the quasiparticle dephasing length at finite temperatures at $\nu = 5/2$.³⁴ In this paper, we apply our model and methods to the $\nu = 2/3$ FQH system.

In this model, we consider a 2DEG confined to a plane with rotational symmetry. There is a neutralizing background charge distributed uniformly on a parallel disk of radius R at a distance d above the 2DEG (see Fig. 1 of Ref. 10 for an illustration). The total charge of the disc is $N_e e$, where N_e is the number of electrons confined to the plane and the radius R or, equivalently, the density of the background charge is determined by the filling fraction ν . We consider $\nu = N_e/N_\Phi = 2N_e l_B^2/R^2$, where l_B is the magnetic length and N_Φ is the number of flux quanta enclosed in the disc. The distance d parameterizes the strength of the electron confining potential due to attraction from background charge, which becomes weaker as d increases. We assume the electrons are spin-polarized, which is the case in strong magnetic fields. In the second quantization language, the Hamiltonian is written as:

$$H_C = \frac{1}{2} \sum_{\{m_i\}} V_{m_1 m_2 m_3 m_4} c_{m_1}^+ c_{m_2}^+ c_{m_4} c_{m_3} + \sum_m U_m c_m^+ c_m \quad (1)$$

where the Coulomb matrix elements $V_{\{m_i\}}$ are

$$V_{\{m_i\}} = \int d^2 r_1 \int d^2 r_2 \phi_{m_1}^*(\vec{r}_1) \phi_{m_2}^*(\vec{r}_2) \frac{e^2}{\epsilon r_{12}} \phi_{m_3}(\vec{r}_1) \phi_{m_4}(\vec{r}_2), \quad (2)$$

and the background confining potential U_m as a function of d is

$$U_m = \frac{N_e e^2}{\pi R^2 \epsilon} \int d^2 r \int_{\rho < R} d^2 \rho \frac{|\phi_m(\vec{r})|^2}{\sqrt{|\vec{r} - \vec{\rho}|^2 + d^2}}. \quad (3)$$

Here ϵ is the dielectric constant. We use the symmetric gauge $\vec{A} = (-\frac{By}{2}, \frac{Bx}{2})$; the single-particle wave function ϕ_m in the lowest Landau level is:

$$\phi_m(z) = (2\pi 2^m m!)^{-1/2} z^m e^{-|z|^2/4}. \quad (4)$$

Throughout the paper, we use the magnetic length l_B as length unit and $e^2/\epsilon l_B$ as energy unit.

It is often convenient to cast the Coulomb matrix elements into a weighted sum of pseudopotentials introduced by Haldane.³⁶ One of the advantages of expressing two-body interactions in terms of pseudopotentials

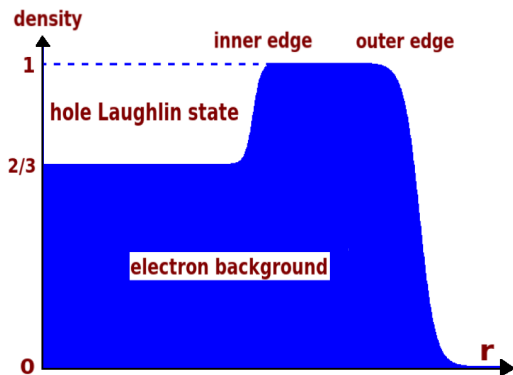


FIG. 1: (color online) Schematic picture of electron density profile along radial direction of a $\nu = 2/3$ FQH droplet. We assume there is a hole Laughlin state embedded in the $\nu = 1$ electron background. Therefore, there are two interfaces: one is between the $1/3$ hole Laughlin state and the integral filling background and the other is between the $\nu = 1$ integer quantum Hall droplet and the vacuum.

is that the Laughlin states become exact ground states for specific pseudopotential Hamiltonians; for example at filling fraction $\nu = 1/3$, with hard-core interaction between electrons (in Haldane’s pseudopotential language, $V_m = \delta_{1,m}$) and in the absence of confining potential, the Laughlin state³⁷

$$\Psi_{1/3}(z_1, \dots, z_N) = \prod_{i>j} (z_i - z_j)^3 \exp\left\{-\frac{1}{4} \sum_{i=1}^N |z_i|^2\right\} \quad (5)$$

is the exact ground state with zero energy, which exists in the subspace of total angular momentum $M = 3N_e(N_e - 1)/2$, for N_e electrons in at least $N_{orb} = 3N_e - 2$ orbitals.

III. GROUND STATE QUANTUM NUMBERS

To begin our study on the $\nu = 2/3$ system, we ask to what extent we can conclude that the ground state of the semi-realistic model can be described by the particle-hole conjugate of the $1/3$ Laughlin state on an IQH background. The schematic profile of the electron density is shown in Fig. 1 in which we neglect the density oscillation of the Laughlin state for holes near its edge (see realistic curves in Fig. 4 for details). Suppose the system contains N_e electrons filling up to the N_I -th orbital (with single particle angular momentum $m = 0, 1, \dots, N_I - 1$). According to this picture, we have two droplets: N_I electrons fill the lowest Landau level (LLL) and form a $\nu_I = 1$ IQH state; in addition, $N_h = (N_I - N_e)$ holes form a $\nu_h = 1/3$ hole Laughlin state. The total angular momentum for such a state is

$$M = \frac{N_I(N_I - 1)}{2} - \frac{3(N_I - N_e)(N_I - N_e - 1)}{2}. \quad (6)$$

To reveal such a state in a microscopic calculation, one needs $N_{orb} \geq N_I$ orbitals. For example, with $N_e = 20$

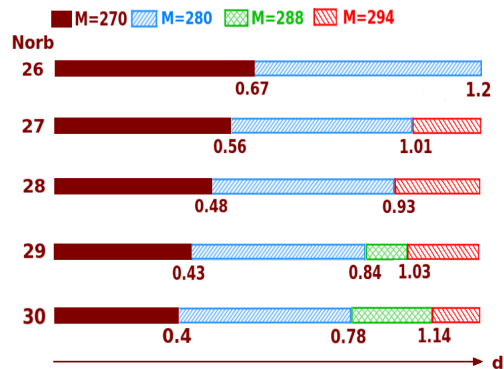


FIG. 2: (color online) Phase diagram for systems with 20 electrons at filling factor $\nu = 2/3$, as a function of number of single electron orbitals N_{orb} and background charge distance d . The ground state total angular momentum M changes as d increases. Angular momenta $M = 270, 280, 288,$ and 294 correspond to 5-, 6-, 7-, and 8-hole Laughlin ground states respectively. However the $M=294$ state with $N_{orb} = 27$ is expected to be a stripe state which can be described by $|\Psi_{SP}\rangle = |011111100000111111111111\rangle$.

electrons filling $N_I = 26$ orbitals, we have a 6-hole Laughlin droplet (filling the innermost 16 orbitals) and a $\nu_I = 1$ IQH droplet (filling all 26 orbitals). The total angular momentum of the state is $M = 280$. We note that for the specific system the average filling fraction is somewhat different from $\nu = 2/3$, due to the higher density near the edge.

If the hole-droplet picture is correct, one can possibly (but not necessarily for energetic reasons) find that the global ground state of the semi-realistic model has a total angular momentum $M = 280$, if 20 electrons are distributed in $N_{orb} \geq N_I = 26$ orbitals.

We study the global ground state of a system of 20 electrons with various d and N_{orb} (which serves as an additional hard edge confinement). We plot the results in Fig. 2. When the distance of the background charge d increases, the confining potential becomes weaker and the total angular momentum of the global ground state increases and goes through steps at $M = 270, 280, 288,$ and 294 . According to Eq. (6), these states correspond to $N_h = 5, 6, 7,$ and 8 holes, respectively. Unlike the Laughlin or Moore-Read Pfaffian cases where M is uniquely determined by the number of electrons and a change of M is an indication of instability,^{31,33} here we have a series of “good” ground states, since the number of electrons only fixes the difference between the IQHE droplet and the hole droplet. In other words, the two edges can move simultaneously to respond to the change of edge confining potential. In this paper, we will focus on the 6-hole state, although the results should be general enough for other cases.

The agreement between the actual series of ground state angular momenta and the prediction of Eq. (6) suggests that the picture of a Laughlin hole droplet em-

bedded in an IQH droplet is a good description of the ground states at $\nu = 2/3$. In the following sections we will present more evidence that this is indeed true for most cases. However, we would like to point out an exception here. The quantum number $M = 294$ is consistent with an 8-hole state. But according to earlier discussion, we need $N_{orb} \geq 28$ orbitals to accommodate this state. The reader may have already noticed that it also appears in the $N_{orb} = 27$ case. This contradiction suggests that there is another state (or phase) that is competing with the hole-droplet picture. In fact, it even suppresses the 7-hole state ($M = 288$). Analysis of the electron occupation number suggests that this state is likely a stripe state. We can use a fermionic occupation number configuration to represent the state as $|\Psi_{SP}\rangle = |011111100000111111111111\rangle$, where the string of 0s and 1s represents the occupation number of the corresponding single-particle orbital (from the left $m = 0, 1, \dots, N_{orb} - 1$). The stripe state is more compact than the 8-hole state and is expected to be energetically more favorable for the restricted case with $N_{orb} = 27$. To confirm this and to quantify the trend from $N_{orb} = 27$ to 30, we calculate the overlap between the ground state with $M = 294$ and $|\Psi_{SP}\rangle$ and find that the ground state indeed has a large overlap ($|\langle\Psi_{SP}|\Psi_{M=294}\rangle|^2 = 25.4\%$) with a stripe state when $N_{orb} = 27$ and $d = 1.2l_B$. This overlap decreases as we increase the number of orbitals to 19.4% in 28 orbitals, 16.2% in 29 orbitals, and 8.2% in 30 orbitals, suggesting the ground state for large enough N_{orb} is not the stripe phase, but possibly the 8-hole state. Note that for well-defined overlap, we need to add the proper number of 0s to the right of the occupation number configuration $|\Psi_{SP}\rangle$.

IV. GROUND STATE WAVE FUNCTIONS AND OVERLAPS

In this section we study the ground state wave functions at $\nu = 2/3$ and show that they are consistent with the picture of a $\nu_h = 1/3$ hole droplet on top of a $\nu_e = 1$ electron droplet. For comparison between the two, we construct variational wave functions for $\nu = 2/3$ ground states by particle-hole conjugation of electron Laughlin states and calculate overlaps between them. To be specific, we target the 6-hole ground state with $M = 280$. We first fill the lowest 26 single-particle LLL orbitals to obtain an IQH state, which can be represented by a string of single-particle occupation numbers $|111 \dots 111\rangle$. Then, we construct a 6-hole Laughlin wave function in the following manner. A 6-electron Laughlin state, which is partially occupying the lowest 16 orbitals, can be written as

$$|L_{16}^6\rangle = \prod_{1 \leq i < j \leq 6} (z_i - z_j)^3, \quad (7)$$

where we have omitted a normalization constant and the Gaussian factor $\exp\{-\sum_i |z_i|^2/4\}$. We note that the

N_{orb}	26	27	28	29	30
Size of HS	1123	10867	54799	184717	473259
$ \langle\Psi_{gs} \bar{L}_{16}^6\rangle_{N_{orb}}^{20} ^2$	0.9401	0.7868	0.7012	0.6431	0.6011

TABLE I: Overlaps between 20-electron ground states with $M = 280$ and $d = 0.7l_B$ and the particle-hole conjugate of the 6-electron Laughlin state obtained from the hard-core Hamiltonian for several different numbers of orbitals N_{orb} . In the case of $d = 0.7$, the ground state with $M = 280$ is the global ground state for all cases in Fig. 2. The Hilbert subspace (HS) size for $M = 280$ increases rapidly when N_{orb} increases from 26 to 30 by about 450 times; however the overlap decreases slowly, indicating the robustness of the state.

Laughlin state is a many-body wave function and can be written, symbolically in the second quantization form, as

$$|L_{16}^6\rangle = \sum_{\{i_n\}} \alpha_{\{i_n\}} c_{i_1}^\dagger c_{i_2}^\dagger c_{i_3}^\dagger c_{i_4}^\dagger c_{i_5}^\dagger c_{i_6}^\dagger |0\rangle_{16}, \quad (8)$$

where

$$|0\rangle_{16} = |000 \dots 000\rangle_{16} \quad (9)$$

is the vacuum in 16 orbitals. Therefore, the 6-hole droplet embedded in 16 orbitals is

$$|\bar{L}_{16}^6\rangle = \sum_{\{i_n\}} \alpha_{\{i_n\}} c_{i_1} c_{i_2} c_{i_3} c_{i_4} c_{i_5} c_{i_6} |111 \dots 111\rangle_{16}, \quad (10)$$

which contains 10 electrons. After adding the additional 10 filled orbitals, we have a many-body variational wave function for 20 electrons in 26 orbitals, which we denote as $|\bar{L}_{16/26}^6\rangle_{20} = |\bar{L}_{16}^6\rangle \otimes |1111111111\rangle_{10}$. For $N_{orb} > 26$, we can add trailing 0s for the empty orbitals at the edge accordingly, which we denote as $|\bar{L}_{16/N_{orb}}^6\rangle_{20}$. We compare $|\bar{L}_{16/N_{orb}}^6\rangle_{20}$ to the ground state of our semi-realistic model with $d = 0.7l_B$, at which all ground states for $N_{orb} = 26-30$ have $M = 280$, as shown in Fig. 2. Table I shows the overlap between the global ground state $|\Psi_{gs}\rangle$ in different numbers of orbitals and the 6-hole variational wave function $|\bar{L}_{16/N_{orb}}^6\rangle_{20}$. As N_{orb} varies from 26 to 30, the dimension of the Hilbert space increases by a factor of about 450, while the overlap still survives at about 60%. The decrease is largely due to the fact that the outer edge is no longer sharp as the angular momentum cut-off $(N_{orb} - 1)$ increases.

In addition, the strength of the confining potential due to neutralizing background charge also affects, though in a minor way, the overlap between the $\nu = 2/3$ electron ground state and the variational wave function $|\bar{L}_{16/N_{orb}}^6\rangle_{20}$. Fig. 3 shows that, for the regime in which the total angular momentum of the global ground state is $M = 280$, the overlap for 20 electrons in 26 orbitals decreases from 0.94 to 0.93 as d increases from 0.67 to 1.2. As the distance d between the 2DEG and the background charge increases, the confining potential the electrons experience becomes weaker. The electron wave function can expand, leading

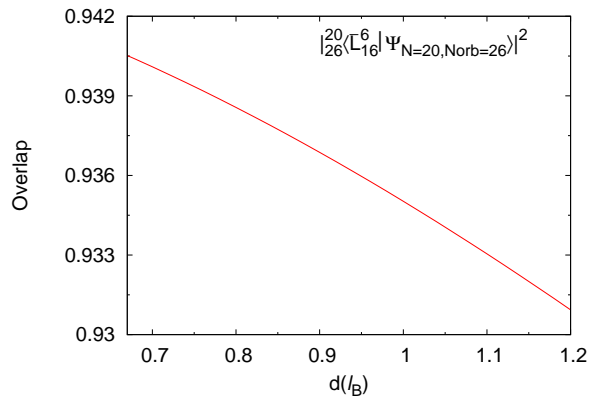


FIG. 3: Overlap between the 20-electron ground state in 26 orbitals and the particle-hole conjugate of the 6-electron Laughlin state as a function of d . The decrease of the overlap indicates that the particle-hole conjugate Laughlin state favors smaller d , i.e., stronger confinement.

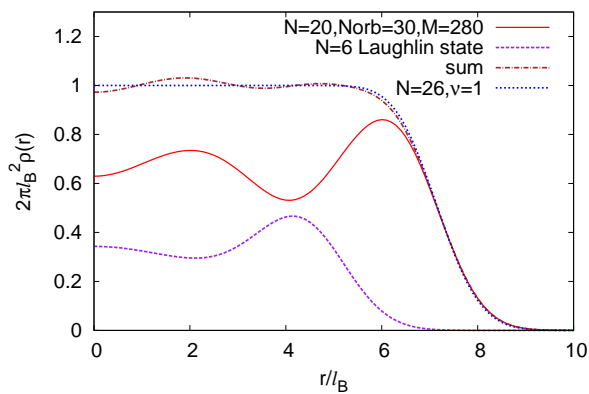


FIG. 4: (color online) Density profiles for the 6-electron Laughlin state, the 20-electron ground state in 30 orbitals with $M = 280$ and $d = 0.7l_B$, the sum of them, and the 26-electron IQH state. The sum is almost the same as the density of IQH.

to a smaller overlap. This is consistent with the N_{orb} dependence, in the sense that the hole-droplet ground state favors stronger confinement. But since the range of d for a ground state with a certain number of holes is narrow, we can neglect the 1% change.

An alternative way to compare states is to contrast the electron density profiles (though it is possible that two wave functions with identical density profiles can be orthogonal to each other). In Fig. 4, we plot the density profile of a 6-electron Laughlin state and that of the 6-hole ground state obtained by exact diagonalization of a system of 20 electrons in 30 orbitals at $d = 0.7l_B$. To compare, we plot the sum of the density profiles of the Laughlin state and the 6-hole state, together with the density profile of an IQH state with 26 electrons. It is clear that the density sum is almost the same as the den-

sity of the IQH state, except for small oscillations which can be attributed to the long-range Coulomb interaction in the semi-realistic microscopic model.

V. EDGE EXCITATIONS

The analysis that can further confirm the picture that the $\nu = 2/3$ state is a Laughlin hole-droplet embedded in an IQH background is the study of edge excitations. In topological systems like FQH liquids, edge states have been demonstrated to be very effective and essential probes of the bulk topological order in both theoretical calculations and experiments. As shown in Fig.1, one expects two counter-propagating edge modes originating from the two edges at $2/3 \rightarrow 1$ and $1 \rightarrow 0$.^{11,12,13} In the same spirit as the analysis in Refs. 33 and 34, we can label each low-energy edge excitation by two sets of occupation numbers $\{n_L(l_L)\}$ and $\{n_R(l_R)\}$ for the inner and outer edge modes with angular momenta l_L, l_R and energies ϵ_L, ϵ_R , respectively. $n_L(l_L)$ and $n_R(l_R)$ are non-negative integers. The angular momentum and energy of an edge excitation, measured relatively from those of the ground state, are

$$\Delta M = - \sum_{l_L} n_L(l_L) l_L + \sum_{l_R} n_R(l_R) l_R, \quad (11)$$

$$\Delta E = \sum_{l_L} n_L(l_L) \epsilon_L(l_L) + \sum_{l_R} n_R(l_R) \epsilon_R(l_R). \quad (12)$$

For the latter we assumed absence of interactions among the excitations. The negative sign in Eq. (11) indicates the inner edge mode is propagating in the opposite direction to the outer edge mode.

In Fig. 5, we plot the low-energy spectrum for 20 electrons in 28 orbitals at $d = 0.5l_B$, whose global ground state has $M = 280$. The edge states are labeled by red bars based on the analysis we will discuss in the following paragraphs. Here we first point out that the inner edge excitations have negative ΔM and are separated by an energy gap from other states (presumably bulk states) in each angular momentum subspace. The number of these inner edge states (including the ground state) are 1, 1, 2, 3, and 5 for $\Delta M = 0-4$, as predicted by the chiral boson edge theory.¹³ They have significant overlap with a 6-hole Laughlin droplet with corresponding edge excitations embedded in a 26-electron IQH background. On the other hand, the outer edge excitations ($\Delta M > 0$) have higher excitation energies and are mixed with bulk states. In particular, for $\Delta M = 1$, the edge state is the second lowest eigenstate in the $M = 281$ subspace. The state has a large overlap (62.7%) with the 6-hole Laughlin droplet embedded in the 26-electron IQH state with an edge excitation at $\Delta M = 1$. Obviously, the outer edge mode has a larger velocity than the inner edge mode, consistent with the different charge density associated with the edge modes.

To identify the inner edge excitations, we compare the edge spectrum to that of a 6-electron system at $\nu = 1/3$,

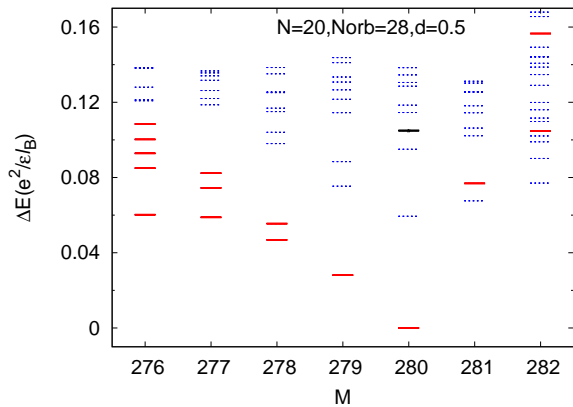


FIG. 5: (color online) Low-energy spectrum for 20 electrons in 28 orbitals with $d = 0.5$. The inner and outer edge states are labeled by red bars and the simplest combination of the two is labeled by a black bar. Its energy (0.1049) is roughly the sum of the two lowest excitation energies for the two modes: 0.02807(inner)+0.07687(outer). This state has a moderately large overlap(0.3959) with the particle-hole conjugate of a 6-electron Laughlin state with $\Delta M = 1$ edge excitation and embedded in the IQH edge state with $\Delta M = 1$: $|\bar{L}_{17}^6(\Delta M = 1) \cdots 1101 \rangle$.

with the neutralizing background charge at the same distance from the 2DEG. In Fig. 6, we plot side-by-side the $\nu = 1/3$ and the $\nu = 2/3$ edge spectra, both with $d = 0.5l_B$. The edge states are labeled by red bars. From the comparison, one clearly sees that the $\nu = 2/3$ state and the $\nu = 1/3$ state have similar edge excitations, but along opposite directions. The one-to-one correspondence of the edge excitations in the two cases can be established by studying overlaps of the corresponding pairs. Of course, the overlap that we really calculated is the overlap between the eigenstate for $\nu = 2/3$ and the corresponding particle-hole conjugated state for $\nu = 1/3$ embedded in the 26-electron IQH background. To minimize the influence from the momentum cut-off, we choose 6 electrons in 22 orbitals with the same background ($d = 0.5l_B$) for $1/3$ filling. The results of the overlap calculation are summarized in Table II. The overlap becomes smaller as we go to higher energy, but remains above 40% up to $|\Delta M| = 4$. Overlaps between other pairs of states are significantly smaller.

In order to identify edge excitations with positive ΔM , we need to consider the IQH edge excitations of the outer edge. A 26-electron IQH ground state in 28 orbitals can be represented by occupation numbers $|11 \cdots 11100\rangle$, with 26 consecutive 1s followed by two 0s. So after adding a 6-hole Laughlin hole droplet, we denote the ground state as $|\bar{L}_{16}^6 \cdots 11100\rangle$ for convenience, although the many-body variational state cannot be written as a single occupation number string (i.e., a Slater determinant). In the same spirit, we can construct and denote variational wave functions with IQH edge excitations as $|\bar{L}_{16}^6 \cdots 11010\rangle$ for $\Delta M = 1$, $|\bar{L}_{16}^6 \cdots 11001\rangle$ and

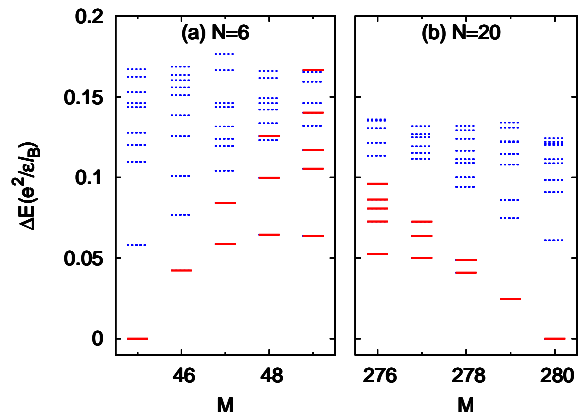


FIG. 6: (color online) Comparison of the low energy excitation spectrum of the $\nu = 1/3$, 6-electron Laughlin edge states (6 electrons in 22 orbitals with Coulomb interaction, $d = 0.5l_B$) (a) and $\nu = 2/3$, 6-hole Laughlin edge states (20 electrons in 28 orbitals, $d = 0.5l_B$) (b). The edge states are labeled by red bars. The overlaps between these edge states are shown in table II.

$|\bar{L}_{16}^6 \cdots 10110\rangle$ for $\Delta M = 2$ in order to emphasize the excitation at the outer edge. We calculate the overlap between the variational wave function $|\bar{L}_{16}^6 \cdots 11010\rangle$ and the states in $M = 281$ subspace. The largest we find is the second state, $|\langle \Psi_{M=281_2} | \bar{L}_{16}^6 \cdots 11010 \rangle|^2 = 0.6272$, which we identify as the outer edge excitation. Similarly for $\Delta M = 2$, we identify the fifth state, which has $|\langle \Psi_{M=282_5} | \bar{L}_{16}^6 \cdots 10110 \rangle|^2 = 0.1896$, and the seventeenth state, which has $|\langle \Psi_{M=282_{17}} | \bar{L}_{16}^6 \cdots 11001 \rangle|^2 = 0.1794$, as edge excitations. We note the overlap already becomes small for $\Delta M = 2$, indicating significant mixing between the edge states and bulk states. This is not surprising since, for the small system we consider, there is no gap protecting the edge states.

Eqs. (11) and (12) suggest that there are also composite excitations that are combinations of these two counter-propagating edge modes. The simplest one is the combination of the edge states with $\Delta M = -1$ and $\Delta M = 1$, which resides in the $M = 280$ subspace. Intuitively, we can construct a variational wave function by particle-hole conjugating a 6-electron Laughlin state with the $\Delta M = 1$ edge excitation and embedding it in the IQH state with $\Delta M = 1$, which we denote as $|\bar{L}_{17}^6(\Delta M = 1) \cdots 11010\rangle$. We find that the fourth state in the $M = 280$ subspace has the largest overlap (about 0.3959) with $|\bar{L}_{17}^6(\Delta M = 1) \cdots 11010\rangle$; meanwhile, its excitation energy ($\Delta E = 0.1049$) is roughly the sum of the excitation energy of the $\Delta M = 1$ edge state ($\Delta E = 0.07687$) for the outer edge and the $\Delta M = -1$ state ($\Delta E = 0.02807$) for the inner edge, confirming Eq. (12).

Fig. 7 compares the dispersion curves and corresponding edge velocities for both the inner edge mode of the 20-electron droplet at $\nu = 2/3$ and the edge mode of a 6-electron Laughlin droplet at $\nu = 1/3$ with different

	1	2	3	4	5
$ \langle \Psi_{M=45} \Psi_{M=280} \rangle ^2$	0.7527 _(1 1)				
$ \langle \Psi_{M=46} \Psi_{M=279} \rangle ^2$	0.6615 _(1 1)				
$ \langle \Psi_{M=47} \Psi_{M=278} \rangle ^2$	0.7003 _(1 1)	0.5814 _(2 2)			
$ \langle \Psi_{M=48} \Psi_{M=277} \rangle ^2$	0.7098 _(1 1)	0.6147 _(2 2)	0.5083 _(3 3)		
$ \langle \Psi_{M=49} \Psi_{M=276} \rangle ^2$	0.7180 _(1 1)	0.6238 _(2 2)	0.6000 _(3 3)	0.4999 _(5 4)	0.4130 _(10 5)

TABLE II: The overlaps between the particle-hole conjugated 6-electron edge states (in 22 orbitals with $d = 0.5l_B$; Fig. 6(a)) and the 20-electron inner edge states (in 28 orbitals with $d = 0.5l_B$; Fig. 6(b)). The subscript $\langle n|m \rangle$ means this is the overlap between the n 'th state in the former subspace and the m 'th state in the later subspace.

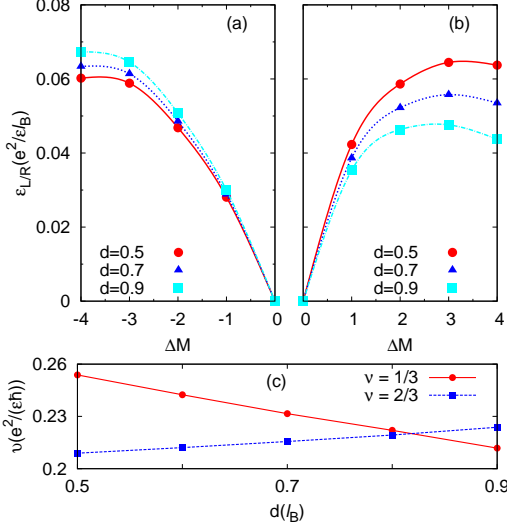


FIG. 7: (color online) The dispersion relation of the inner edge mode for 20 electrons in 28 orbitals at $\nu = 2/3$ (a) and the edge mode of a 6-electron Laughlin droplet in 20 orbitals at $\nu = 1/3$ (b) with different background confinement potentials. The evolutions of the edge velocities as a function of d are plotted in (c). It can be seen that the velocity of the counter-propagating edge mode in the hole Laughlin state crosses that of the electron Laughlin state at around $d = 0.82l_B$ and the velocity of the electron Laughlin state has an opposite response to the change of the background confinement to the hole Laughlin state.

background confinement. The velocity of an edge mode is defined as $v = |d\epsilon(k)/dk|$. The edge excitation with angular momentum ΔM measured from the ground state is related to the edge linear momentum $k = \Delta M/R$, where $R = \sqrt{3N_e}l_B$ is the radius of the N -electron FQH droplet at $\nu = 2/3$ and $R = \sqrt{6N_e}l_B$ for $\nu = 1/3$. Here we smear the difference of the radius between the inner and outer edge of $\nu = 2/3$. We find the velocity of the electron liquid v_e is larger than the corresponding velocity v_h for the hole droplet of the $\nu = 2/3$ FQH state at small d (strong confinement), while v_e is smaller than v_h at large d (weak confinement). The crossing happens at around $d = 0.82l_B$. At $d = 0.5l_B$, the velocity of the electron edge is about $0.25e^2/(\epsilon\hbar)$, while the velocity of the hole

edge mode is about $0.22e^2/(\epsilon\hbar)$. As d increases, v_e decreases (roughly linearly) because the edge confinement is weaker and electrons tend to move out. However, v_h increases linearly with d . Therefore, the symmetry correspondence between the electron droplet and the hole droplet is not exact in the presence of edge confinement.

Meanwhile, in Fig. 5, we pointed out that the second lowest eigenstate in the $M = 281$ momentum subspace is the outer edge state at $d = 0.5l_B$. We can expect that the excitation energy of the edge state decreases with d and may drop below that of the lowest energy state (presumably a bulk state). This is indeed the case, as illustrated in Fig. 8. When increasing the distance d to the neutralizing charge background, we find an anticrossing behavior of the lowest two eigenstates, as their energy difference $\Delta E = E_2 - E_1$ shows a minimum at the crossing scale $d_c = 0.84l_B$. Overlap calculations reveal that below this d_c , the lowest-energy state has a smaller overlap with the corresponding variational wave function of the edge state ($|\bar{L}_{16}^6 \dots 11010\rangle$) than the second lowest state. On the contrary, above d_c , the lowest-energy state has a larger overlap with the variational edge state, which can be regarded as the ground state with an $\Delta M = 1$ outer-edge IQH excitation.

Fig. 9(a) shows the edge dispersion curves for both the inner and the outer edge modes for different background confinement. Similar to the edge mode of the electron Laughlin state, the velocity of the outer edge mode of the $\nu = 2/3$ FQH droplet decreases linearly as d increases, as plotted in Fig. 9(b). At $d = 0.5l_B$, the velocity of the outer edge mode is about $0.596e^2/(\epsilon\hbar)$, slightly smaller than 3 times the inner edge velocity. In this case the small deviation from 3 suggests the two edges may be weakly coupled.

We conclude the section by pointing out that we can identify two edge modes for a $\nu = 2/3$ FQH droplet, propagating along opposite directions. The outer edge velocity is larger than the inner edge velocity. The outer and inner edge modes originate from electron and hole droplets, respectively, and show opposite dependence on the strength of the edge confining potential, which breaks the particle-hole symmetry.

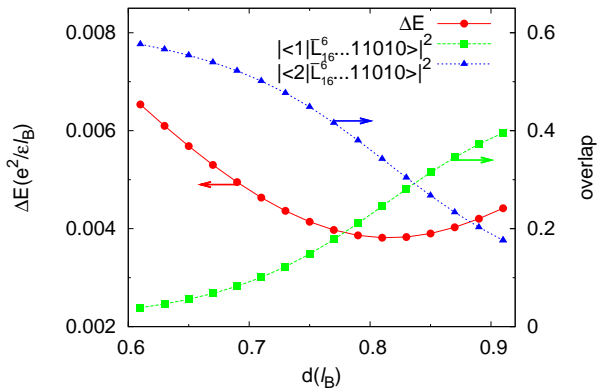


FIG. 8: (color online) The energy gap (red circle point line) $\Delta E = E_2 - E_1$ and the overlap between the integral edge state $|\bar{L}_{16}^{6\dots 11010}\rangle$ and the first two lowest states (square and triangular point line) in $M=281$ subspace as a function of d . The energy gap reaches its minima and the overlap has a crossover between the the first state and the second state at around $d_c = 0.84l_B$ indicating that the first state becomes the outer edge state after $d > d_c$.

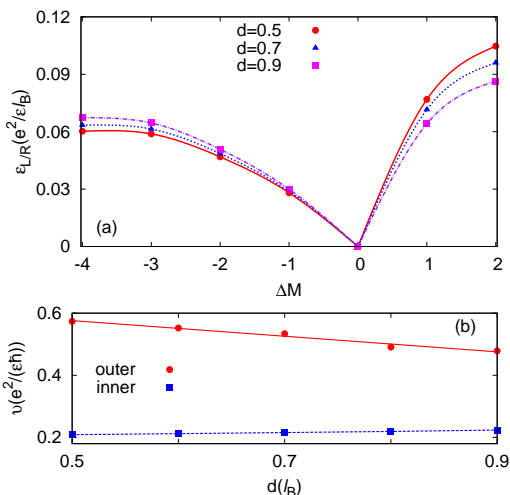


FIG. 9: (color online) The dispersion curves of a $\nu = 2/3$ FQH droplet with 20 electrons in 28 orbitals (a) for both the inner and outer edge modes at different d 's. As in the 6 electron Laughlin state, the velocities of the outer edge mode decrease linearly as a function of d and have larger velocities than the inner edge (b) in the whole parameter range where the global ground state resides in the $M=280$ subspace.

VI. PARTICLE-HOLE TRANSFORMATION

The Laughlin state is the exact zero-energy state of a special two-body Hamiltonian with hard-core interaction. In this section we use particle-hole transformation to construct Hamiltonians that make the hole Laughlin states (which we used as variational ground states in previous sections) exact ground states. As we are going

to show below, such Hamiltonians include not only the same hard-core interaction but also an additional one-body term in the electron basis.

We start by considering a generic two-body Hamiltonian in terms of *hole* operators:

$$H_h = \frac{1}{2} \sum_{\{m_i=0\}}^{N_{orb}-1} V_{m_1 m_2 m_3 m_4} h_{m_1}^+ h_{m_2}^+ h_{m_4} h_{m_3}, \quad (13)$$

where the hole operators h^+ and h are related to electron operators: $h^+ = c$ and $h = c^+$. It is straightforward to express the same Hamiltonian in terms of electron operators:

$$H_h = \frac{1}{2} \sum_{\{m_i=0\}}^{N_{orb}-1} V_{m_1 m_2 m_3 m_4} c_{m_4}^+ c_{m_3}^+ c_{m_1} c_{m_2} - \sum_m \bar{U}_m c_m^+ c_m + \text{const.}, \quad (14)$$

where

$$\bar{U}_m = \sum_n \{V_{nmnm} - V_{nmnm}\} \quad (15)$$

is the Hartree-Fock self-energy of the state m when all the N_{orb} orbitals are occupied by electrons. Thus, in the electron basis we get the same two-body interaction *plus* a one body potential, which is *attractive* if the two-body potential is repulsive.

From now on we focus on the specific short-range (hard-core) interaction that corresponds to Haldane pseudopotential $V_m = \delta_{1,m}$ for H_h . After diagonalizing the Hamiltonian H_h with $N = 20$ electrons in $N_{orb} = 28$, we obtain the energy spectrum in Fig. 10. It is worth pointing out that since there is no edge confinement other than the momentum cut-off due to the choice of N_{orb} , we have $N_h = N_{orb} - N = 8$ holes in the system. Not surprisingly, the largest angular momentum of the degenerate ground states is $M_0 = 294$, as expected from Eq. (6), with $N_l = N_{orb} = 28$ and $N_e = 20$. This is the densest ground state configuration for holes and is thus incompressible. For $\Delta M = M - M_0 = -1, -2, \dots, -5$, we find the ground state degeneracy in each subspace is $n(\Delta M) = 1, 2, 3, 5, \text{ and } 7$, respectively. This is precisely the number expected for the Laughlin droplet (except for this case, the momentum is negative), as generated by

$$\sum_{\Delta M} n(\Delta M) q^{\Delta M} = \prod_{m=1}^{\infty} \frac{1}{1 - q^{-m}}. \quad (16)$$

In the spirit of Refs. 33 and 34, a mixed Hamiltonian that contains both the Coulomb Hamiltonian H_C used in earlier sections and the above hard-core Hamiltonian H_h parameterized by λ is considered:

$$H = \lambda H_h + (1 - \lambda) H_C. \quad (17)$$

The idea here is that the hard-core Hamiltonian H_h raises the energy of bulk excitations while having little effect on

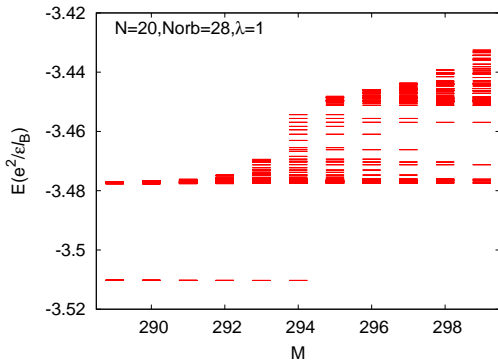


FIG. 10: (color online) The energy spectrum of the P-H conjugated Hamiltonian with hard-core interaction (Eq. (14)) for 20 electrons in the 28 orbitals. M is the total angular momentum for the 20 electrons. The first 50 energy levels are plotted for each M . The lowest energy states (they should be the exact zero energy state if we include the constant term) at $M=294, \dots, 289$ are degenerate with degeneracy 1,1,2,3,5,7.

the edges states, thus its presence helps separate the two energetically. Fig. 11 shows the energy spectrum for 20 electrons in 28 orbitals in the pure Coulomb case ($\lambda = 0$) and a mixed case ($\lambda = 0.5$). Although the ground state of H_h for 20 electrons in 28 orbitals is the 8-hole Laughlin state, for the mixed Hamiltonian above we obtain a different ground state with the same quantum number as the 6-hole Laughlin state ($M = 280$). This is because the neutralizing background charge at $d = 0.9$ serves as a repulsive potential to the holes that pushes two holes to the outer edge. It is clear that edge excitations show up at lower energies for the case $\lambda = 0.5$. In particular, overlap calculations indicate that in the case of pure Coulomb interaction with $\lambda = 0$, the third state in $M=280$ subspace is the simplest combination state which has the largest overlap (0.194) with $|\bar{L}_{17}^6(\Delta M = 1) \dots 11010\rangle$, while in the case of the mixed Hamiltonian with $\lambda = 0.5$, it is the second state in $M=280$ subspace that has the largest overlap (0.296) with $|\bar{L}_{17}^6(\Delta M = 1) \dots 11010\rangle$. Therefore, the mixing of the hard-core Hamiltonian indeed has the effect of separating the band of edge states from the bulk states.

VII. LAYER THICKNESS

One improvement in the semi-realistic model is to consider the effect of finite electron layer thickness. In real experimental samples, quasi-two-dimensional electrons are confined in the GaAs quantum well, whose width can be as large as 30 nm or a few magnetic lengths. Since the vertical motion of electrons is suppressed at low temperatures, the quasi-2DEG can be approximated, to the lowest order, by an ideal 2DEG located at the peak of the wave function in the perpendicular direction. The finite width softens the repulsion between electrons and thus, together with other factors (like higher Landau level),

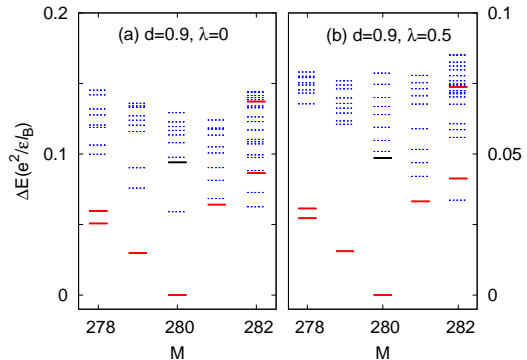


FIG. 11: (color online) The energy spectrum for the pure Coulomb Hamiltonian with $\lambda = 0$ (a) and a mixed Hamiltonian with $\lambda = 0.5$ (b). When $\lambda = 0$ the overlaps between the outer edge states (and ground state) and their corresponding conjugated states are: $|\langle \Psi_{M=280_1} | \bar{L}_{16}^6 \rangle_{26}^{20}|^2 = 0.684$, $|\langle \Psi_{M=281_1} | \bar{L}_{16}^6 \dots 11010 \rangle|^2 = 0.385$, $|\langle \Psi_{M=282_3} | \bar{L}_{16}^6 \dots 10110 \rangle|^2 = 0.133$, $|\langle \Psi_{M=282_{15}} | \bar{L}_{16}^6 \dots 11001 \rangle|^2 = 0.158$; the overlap for the simplest linear combination state is: $|\langle \Psi_{M=280_3} | \bar{L}_{17}^6(\Delta M = 1) \dots 11010 \rangle|^2 = 0.194$. In the case of a mixed Hamiltonian with $\lambda = 0.5$, they are: $|\langle \Psi_{M=280_1} | \bar{L}_{16}^6 \rangle_{26}^{20}|^2 = 0.66$, $|\langle \Psi_{M=281_1} | \bar{L}_{16}^6 \dots 11010 \rangle|^2 = 0.539$, $|\langle \Psi_{M=282_2} | \bar{L}_{16}^6 \dots 10110 \rangle|^2 = 0.218$, $|\langle \Psi_{M=282_{10}} | \bar{L}_{16}^6 \dots 11001 \rangle|^2 = 0.107$, $|\langle \Psi_{M=280_2} | \bar{L}_{17}^6(\Delta M = 1) \dots 11010 \rangle|^2 = 0.296$.

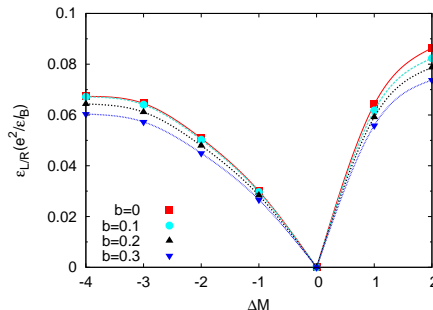


FIG. 12: (color online) The dispersion curves for both the inner edge and the outer edge mode for 20 electrons in 28 orbitals with $d = 0.9l_B$ and different layer thicknesses. The layer thickness softens the interaction between the electrons and reduces the edge mode velocities.

may help stabilize certain fragile FQH states.^{38,39} In this section, we briefly discuss the effects of the 2DEG layer thickness on the velocities of $\nu = 2/3$ edge modes. We use the Fang-Howard^{40,41} variational wave function,

$$Z_0(z) = 2(2b)^{-3/2} z e^{-z/2b}, \quad (18)$$

to model the electron layer thickness effect, where b is a measure of the well thickness. We obtain the same qualitative behavior for an infinite quantum well potential.

We can integrate the Fang-Howard wave function to obtain the renormalized Coulomb interaction in Fourier

space

$$v_{FH}(k) = \frac{e^2}{\epsilon} \frac{1}{8k} \frac{3(kb)^2 + 9kb + 8}{(kb + 1)^3}. \quad (19)$$

In Fig. 12, we show the edge dispersion curves for both the inner and the outer edge modes for a $\nu = 2/3$ FQH droplet of 20 electrons with different layer thicknesses for $d = 0.9$. The ground state angular momentum is again $M = 280$, consistent with the 6-hole Laughlin droplet picture. We find that the velocities of both edge modes are reduced by increasing layer thickness, as expected. This is in contrast to the effects of the confining potential, which modifies edge velocities in an opposite way.

VIII. QUASIPARTICLE

In this section, we demonstrate that both one quasi-hole and one quasiparticle can be excited at the center of the FQH droplet with an additional short-range impurity potential. This section is a natural generalization of similar works by some of the authors for the Laughlin case at $\nu = 1/3$ ³⁵ and for the Moore-Read Pfaffian case.^{33,34}

We follow the previous work³⁵ by using a Gaussian impurity potential $H_W = W_g \sum_m \exp(-m^2/2s^2) c_m^\dagger c_m$ with a finite width $s = 2l_B$ to excite and trap either a quasi-hole or a quasiparticle. We consider a system of 20 electrons at $\nu = 2/3$, whose ground state angular momentum is $M = 280$ for $d = 0.5l_B$. At $W_g = 0.2$ and $W_g = -0.2$, the global ground state resides in the angular momentum subspaces at $M = 286$ and $M = 274$, respectively. The change of the ground state angular momentum M by ± 6 suggests that we have induced a charge $|e|/3$ quasi-hole or a charge $-|e|/3$ quasiparticle at the center of the 6-hole droplet. The density plot for the electron ground state in Fig. 13 confirms the charge depletion and accumulation in the corresponding cases. The increase of the electron ground state angular momentum means a corresponding decrease in the angular momentum of the hole droplet, suggesting a quasiparticle excitation for the hole droplet and thus a quasi-hole excitation for the $\nu = 2/3$ electron ground state, as plotted in Figs. 13(c) and (d). The decrease in angular momentum, on the other hand, suggests a quasiparticle excitation, as plotted in Figs. 13(e) and (f). These excitations are localized at the origin, where we apply the impurity potential, and their presence has no effect on the edge excitation spectrum, since these are Abelian anyons. Roughly speaking, the quasi-hole and quasiparticle excitations induce the same density perturbation on the ground state, except for the opposite signs, suggesting a quasiparticle-quasi-hole symmetry.

IX. CONCLUDING REMARKS

To summarize, we study the ground states, edge, and bulk excitations of $\nu = 2/3$ fractional quantum Hall condensates in a semi-realistic microscopic model. We find

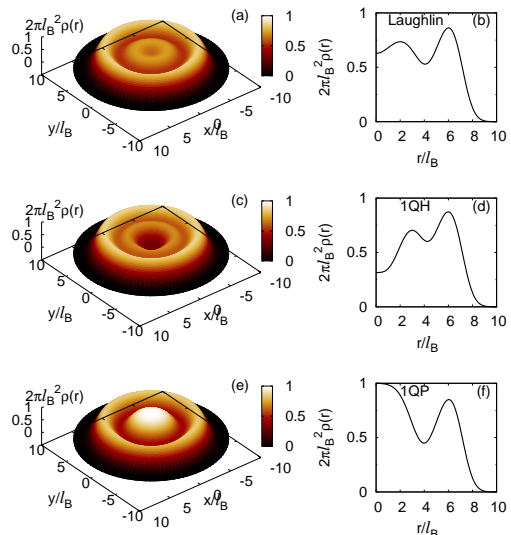


FIG. 13: (color online) The density profile of the $2/3$ state ($1/3$ hole-Laughlin state) and its quasi-hole and quasiparticle excitations. The system contains 20 electrons in 30 orbitals with $d = 0.5l_B$ and the Gaussian tip potential $H_W = W_g \sum_m \exp(-m^2/2s^2) c_m^\dagger c_m$ has a width $s = 2l_B$. (a) and (b) are the density profiles for the ground state with angular momentum $M=280$, (c) and (d) are the density profiles for one quasi-hole state with $M=286$ when $W_g = 0.2$ and (e) and (f) are for one quasiparticle state with $M=274$ and $W_g = -0.2$.

strong numerical evidence that a $\nu = 2/3$ droplet can be regarded as a $\nu_h = 1/3$ Laughlin hole droplet embedded in a larger $\nu_I = 1$ integer quantum Hall droplet. In particular, we find two counter-propagating edge modes, which are associated with the inner edge (the edge of the hole droplet) and the outer edge (the edge of the integer quantum Hall edge). The inner edge mode is well separated from bulk excitations and resembles the edge of a $\nu = 1/3$ electron droplet, except that they propagate in opposite directions and respond oppositely to the edge confining potential, which explicitly breaks the particle-hole symmetry. The outer edge states have higher energy and mix with bulk excitations due to the computational limit on the Hilbert space dimension. The $\nu = 2/3$ quantum Hall droplet also has the same $\pm e/3$ quasiparticle and quasi-hole excitation as a $\nu = 1/3$ Laughlin droplet. These features are robust in the presence of finite electron layer thickness, which softens the Coulomb interaction between electrons.

One of the major advantages of the disk geometry is that we can identify edge modes and determine the velocities of the edge modes. We have previously applied the same method to $\nu = 5/2$ fractional quantum Hall systems and found significant differences in charge and neutral velocities,³⁴ which leads to quite different temperature regimes in which charge $e/4$ and charge $e/2$ quasiparticles can be observed in interference experiments.^{27,42} Similarly, based on comparison with the edge excitations in the $\nu = 1/3$ Laughlin case and in the $\nu = 1$ integer case,

we are able to resolve the edge excitations of the $\nu = 2/3$ case. It is interesting to point out that the outer edge velocity is roughly 3 times that of the inner edge mode velocity, which is about the same as the edge mode velocity of the $\nu = 1/3$ Laughlin liquid with the same Coulomb interaction and a similar confining potential strength due to the neutralizing charge background (Fig. 7c). In general, edge mode velocities are non-universal, depending on details of electron-electron interaction and confining potential. For $\nu = 2/3$, at which there are two counter-propagating edge modes, the velocities further depend on the coupling between the two edge modes affected by interactions and impurities,^{13,15} for example. The fact that we are observing a relatively robust ratio (~ 3) of the outer edge mode velocity to the inner one (consistent with their density changes) suggests that, at the length scale of our finite-size study, the velocities are dominated by the Coulomb interaction strength determined by the electron density change associated with each mode and that the two edge modes are very weakly coupled. We note that, in the thermodynamic limit, the long-range nature of the Coulomb interaction is expected to force the two modes to reorganize into a charge mode and a neutral mode, with the charge mode velocity logarithmically divergent while the neutral mode velocity remains finite in the long wave length limit. The systems size of our study is too small to see this trend.

Another feature of the current calculation is that we consider a semi-realistic confining potential arising from the neutralizing background charge. This, together with long-range interaction between electrons, allows us to compare the energetics of competing states and discuss the qualitative dependence of eigenenergies and edge mode velocities on the confining potential. This is an extremely interesting subject, especially when we have the $\nu = 5/2$ quantum Hall systems in mind. In that

case, there are at least two competing candidates for the ground states, the Moore-Read Pfaffian state and its particle-hole conjugate, the anti-Pfaffian state. They are exactly degenerate, if we neglect the particle-hole symmetry breaking terms, such as the 3-body interaction due to Landau level mixing. As demonstrated in this study, the confining potential is also a relevant symmetry breaking term, which leads to an opposite dependence of the edge mode velocities on this potential. It has been predicted³⁴ that the anti-Pfaffian state is favored in weak confinement (smooth edge) while the Moore-Read Pfaffian state is favored in strong confinement (sharp edge). It is also interesting to point out that for $\nu = 2/3$ the dependence of the edge mode velocity of the inner edge on the confining potential is significantly weaker than that of the outer edge (Fig. 9), suggesting a screening effect by the outer edge on the inner edge to the change of the confining potential.

X. ACKNOWLEDGEMENT

The authors are grateful to Matthew Fisher for discussions and encouragement that initiated this work, and to Kwon Park and Bernd Rosenow for helpful discussions. This work is supported by NSFC Grant No. 10504028 (Z.X.H., H.C. & X.W.) and NSF grants No. DMR-0704133 (K.Y.) and DMR-0606566 (E.H.R.). This research was supported in part by the PCSIRT (Project No. IRT0754). Z.X.H. thanks the Ministry of Education of China for support to visit the NHMFL. X.W. acknowledges the Max Planck Society (MPG) and the Korea Ministry of Education, Science and Technology (MEST) for the support of the Independent Junior Research Group at the Asia Pacific Center for Theoretical Physics (APCTP).

-
- ¹ X.-G. Wen, *Quantum Field Theory of Many-Body Systems* (Oxford University Press, 2004).
- ² V. J. Goldman and B. Su, *Science* **267**, 1010 (1995).
- ³ R. De-Picciotto, M. Reznikov, M. Heiblum, V. Umansky, G. Bunin, and D. Mahalu, *Nature* **389**, 162 (1997).
- ⁴ L. Saminadayar, D. C. Glattli, Y. Jin, and B. Etienne, *Phys. Rev. Lett.* **79**, 2526 (1997).
- ⁵ F. E. Camino, W. Zhou, and V. J. Goldman, *Phys. Rev. Lett.* **95**, 246802 (2005).
- ⁶ F. E. Camino, W. Zhou, and V. J. Goldman, *Phys. Rev. B* **72**, 075342 (2005).
- ⁷ V. J. Goldman, *Phys. Rev. B* **75**, 045334 (2007).
- ⁸ E.-A. Kim, *Phys. Rev. Lett.* **97**, 216404 (2006).
- ⁹ J. J. Palacios and A. H. MacDonald, *Phys. Rev. Lett.* **76**, 118 (1996).
- ¹⁰ X. Wan, E. H. Rezayi, and K. Yang, *Phys. Rev. B* **68**, 125307 (2003).
- ¹¹ A. H. MacDonald, *Phys. Rev. Lett.* **64**, 220 (1990).
- ¹² M. D. Johnson and A. H. MacDonald, *Phys. Rev. Lett.* **67**, 2060 (1991).
- ¹³ X.-G. Wen, *Intl. J. Mod Phys. B* **6**, 1711 (1992).
- ¹⁴ C. L. Kane and M. P. A. Fisher, *Phys. Rev. B* **51**, 13449 (1995).
- ¹⁵ C. L. Kane, M. P. A. Fisher, and J. Polchinski, *Phys. Rev. Lett.* **72**, 4129 (1994).
- ¹⁶ C. L. Kane and M. P. A. Fisher, *Phys. Rev. B* **55**, 15832 (1997).
- ¹⁷ F. D. M. Haldane, *Phys. Rev. Lett.* **74**, 2090 (1995).
- ¹⁸ C. L. Kane and M. P. A. Fisher, *Phys. Rev. B* **52**, 17393 (1995).
- ¹⁹ A. M. Chang, L. N. Pfeiffer, and K. W. West, *Phys. Rev. Lett.* **77**, 2538 (1996).
- ²⁰ U. Zülicke, A. H. MacDonald, and M. D. Johnson, *Phys. Rev. B* **58**, 13778 (1998).
- ²¹ E. V. Deviatov, V. T. Dolgoplov, A. Lorke, W. Wegscheider, and A. D. Wieck, *JETP Letters* **82**, 539 (2005).
- ²² G. Moore and N. Read, *Nucl. Phys. B* **360**, 362 (1991).
- ²³ S.-S. Lee, S. Ryu, C. Nayak, and M. P. A. Fisher, *Phys. Rev. Lett.* **99**, 236807 (2007).
- ²⁴ M. Levin, B. I. Halperin, and B. Rosenow, *Phys. Rev. Lett.*

- 99**, 236806 (2007).
- ²⁵ M. Dolev, M. Heiblum, V. Umansky, A. Stern, and D. Mahalu, *Nature* **452**, 829 (2008).
- ²⁶ I. P. Radu, J. B. Miller, C. M. Marcus, M. A. Kastner, L. N. Pfeiffer, and K. W. West, *Science* **320**, 899 (2008).
- ²⁷ R. L. Willett, M. J. Manfra, L. N. Pfeiffer, and K. W. West, arXiv:0807.0221v1.
- ²⁸ N. Read and E. Rezayi, *Phys. Rev. B* **59**, 8084 (1999).
- ²⁹ W. Bishara, G. A. Fiete, and C. Nayak, *Phys. Rev. B* **77**, 241306 (2008).
- ³⁰ E. V. Deviatov and A. Lorke, arXiv:0803.2612v1.
- ³¹ X. Wan, K. Yang, and E. H. Rezayi, *Phys. Rev. Lett.* **88**, 056802 (2002).
- ³² X. Wan, F. Evers, and E. Rezayi, *Phys. Rev. Lett.* **94**, 166804 (2005).
- ³³ X. Wan, K. Yang, and E. H. Rezayi, *Phys. Rev. Lett.* **97**, 256804 (2006).
- ³⁴ X. Wan, Z.-X. Hu, E. H. Rezayi, and K. Yang, *Phys. Rev. B* **77**, 165316 (2008).
- ³⁵ Z.-X. Hu, X. Wan, and P. Schmitteckert, *Phys. Rev. B* **77**, 075331 (2008).
- ³⁶ F. D. M. Haldane, *Phys. Rev. Lett.* **51**, 605 (1983).
- ³⁷ R. B. Laughlin, *Phys. Rev. Lett.* **50**, 1395 (1983).
- ³⁸ M. R. Peterson, T. Jolicoeur, and S. D. Sarma, *Phys. Rev. Lett.* **101**, 016807 (2008).
- ³⁹ M. R. Peterson and S. Das Sarma, arXiv:0801.4819.
- ⁴⁰ T. Ando, A. B. Fowler, and F. Stern, *Rev. Mod. Phys.* **54**, 437 (1982).
- ⁴¹ F. Stern and S. Das Sarma, *Phys. Rev. B* **30**, 840 (1984).
- ⁴² W. Bishara and C. Nayak, *Phys. Rev. B* **77**, 165302 (2008).